Materials Science & Engineering A 719 (2018) 199–205

Contents lists available at ScienceDirect

Materials Science & Engineering A

journal homepage: www.elsevier.com/locate/msea

Dynamic co-precipitation of α-Mn / $Mg_{12}Ce$ in creep resistant Mg-Sr-Mn-Ce alloys

M. Celikin*, R. Gauvin, M. Pekguleryuz

McGill University, Mining and Materials Engineering, 3610 University St, Wong Bldg, Rm 2140, Montreal, QC, Canada H3A 0C5

ARTICLE INFO

Keywords:
Magnesium alloy
Rare-earth
Creep
Transmission electron microscopy
Dynamic precipitation

ABSTRACT

Quaternary Mg-Sr-Mn-Ce alloys with trace Ce additions exhibit four times lower creep strain than the ternary Mg-Sr-Mn alloys at 200 °C and 50 MPa. Upon thermal exposure, the main phase transformation is the precipitation of both α-Mn and $Mg_{12}Ce$ / α-Mn in intradendritic regions from supersaturated Mg matrix. It was seen that 2D plates of $Mg_{12}Ce$ phases formed with their habit plane perpendicular to $g = 2\bar{1}\bar{1}0$ and affected the size, morphology and orientation of the α-Mn precipitates. 2D plates form obstacles to < a > dislocations impeding basal and prismatic slip. Dynamic co-precipitates of $Mg_{12}Ce$ / α-Mn act a key role in creep strengthening via dislocation pinning.

1. Introduction

Vehicle weight reduction is an important solution for environmental concerns and governs alloy development strategies for automotive applications. The replacement of steel (7.75 – 8.05 g/cm^3) and aluminium (2.70 g/cm^3) powertrain components (engine block and transmission case) with magnesium (1.74 g/cm^3), the lightest structural metal, will enable significant weight reduction. Today, the use of Mg alloys in powertrain components is limited due to the low creep resistance of the most common Mg alloys (AZ91, AM50) [1–3]. The research focus in the last two decades has been on RE alloying additions to Mg for improving the creep resistance at the expense of production cost [4–6]. Hence, limiting the use of RE additions at low concentrations through the combined use of alloying additions is an effective route towards the development of cost-efficient Mg alloys for the industry.

Previous studies by the authors on Mn-bearing Mg-Sr-Mn alloys have shown the important role of α-Mn precipitates dynamically forming from supersaturated α-Mg matrix [7,8] in achieving good creep resistance up to 175 °C. The improvement in creep resistance (~ 10 times lower final strain for Mg-3Sr-2Mn (ε_{final}: 0.124) compared with Mg-3Sr (ε_{final}: 1.275) at 175 °C, 40 MPa after 150 h [7]) is attributed to dislocation pinning by dynamically formed α-Mn precipitates, and an increase in the amount of $Mg_{17}Sr_2$ dendritic phase.

Understanding the effects of minor additions of cerium (Ce) on the creep resistance of ternary Mg-Sr-Mn alloys and the study of their microstructural evolution are the main objectives of this study. There have been previous studies on the effect of Ce on pure Mg. Binary Mg-Ce alloys have the $Mg_{12}Ce$ intermetallic which exists both as coarse interdendritic eutectics and as intradendritic solid state precipitates [5,6,9,10]. It has been shown that it is the dynamically formed intradendritic $Mg_{12}Ce$ precipitate that has a dominant effect on creep resistance rather than the coarse interdendritic $Mg_{12}Ce$ eutectic [6,11]. The removal of the interdendritic phase via solution treatment caused no significant change in the creep properties at 200 °C [4] in Mg-Ce alloys while, the refinement of $Mg_{12}Ce$ precipitate size via Mn additions caused substantial improvement in creep resistance [4–6,12]. Dynamically co-precipitated α-Mn and $Mg_{12}Ce$ phases mutually affect the nucleation and growth of the precipitates leading to both a decrease in precipitate size and an increase in the number of precipitates in ternary Mg-Ce-Mn alloys [6].

The focus in this study is the dynamic precipitates and their role in creep resistance in two quaternary compositions, Mg-5Sr-2Mn-0.5Ce and Mg-3Sr-2Mn-0.5Ce (% wt.) through creep tests and microstructural characterization. A comparison is also provided with creep resistant ternary Mg-(3-5)Sr-2Mn alloys previously studied by the authors.

2. Experimental procedure

Mg-Sr-Mn-Ce alloys were prepared in a Norax induction furnace using pure Sr (99.99 wt%) and pure Ce (99.7 wt%) supplied by HEFA, pure Mg (99.9 wt%) and Mg-Mn (5 wt%) master alloy (Applied Magnesium – formerly Timminco). The alloys were cast into a steel permanent-mold preheated to 400 °C to produce cylindrical bars (of 30 mm diameter) from which tensile creep samples were machined out according to ASTM-E8. Inductively coupled plasma (ICP) analysis was used to determine the chemical composition of the cast bars (Table 1).

* Corresponding author. Present address: University College Dublin, UCD School of Mechanical and Materials Engineering, Belfield, Dublin 4, Ireland.
E-mail addresses: mert.celikin@ucd.ie, mert.celikin@mail.mcgill.ca (M. Celikin), raynald.gauvin@mcgill.ca (R. Gauvin), mihriban.pekguleryuz@mcgill.ca (M. Pekguleryuz).

https://doi.org/10.1016/j.msea.2018.02.041
Received 9 December 2017; Received in revised form 8 February 2018; Accepted 9 February 2018
Available online 10 February 2018
0921-5093/

Table 1
Alloy compositions, wt% (ICP analysis).

Alloy	Designation	Mn	Ce	Sr
Mg-3Sr-2Mn	JM32	2.09	0.06	3.27
Mg-3Sr-2Mn-0.5Ce	JME321	1.90	0.43	3.50
Mg – 5Sr – 2Mn	JM52	1.91	0.06	5.56
Mg – 5Sr – 2Mn – 0.5Ce	JME521	2.01	0.59	6.16

Compositions in this work are presented in wt% unless otherwise stated. Tensile creep tests were conducted under 40–50 MPa stress at a temperature of 175–200 °C on as-cast alloys. For displacement measurements during each creep test, two extensometers (B1-error (ε) ~ < 0.0001 mm/mm) were attached and thermocouples with an error of ± 0.1 °C were connected to the creep specimens for temperature control. Scanning electron microscopy (SEM) analysis was conducted (Hitachi SU3500 SEM at 20 kV) on samples that are ground and polished up to 1200 grid and 1 μm diamond paste respectively. Samples for (scanning) transmission electron microscopy (TEM) investigation were first cut as plates of 1.0 mm thickness, and then ground down to 1200 grid to obtain 0.2 mm thick plates. Discs, 3 mm in diameter, were punched and then Ion-beam Polishing (PIPS) was conducted. TEM analysis was performed using Tecnai G2 F20 TEM at 200 kV and Hitachi SU-8500 SEM was used for STEM analysis for high resolution EDS-mapping.

3. Results and discussion

3.1. Creep behaviour

The creep curves for the tests performed at temperature and stress ranges of 175–200 °C and 40–50 MPa are shown in Fig. 1. Four times lower strain value is obtained in Mg-5Sr-2Mn-0.5Ce i.e. with the addition of a low level of Ce to the ternary Mg-5 Sr-2Mn (Fig. 1a). Sr also has an effect; with the increase in Sr level from 3% to 5%, one order of magnitude improvement in creep resistance (200 °C, 50 MPa, 300–500 h) is achieved. However, it is noted that Ce concentration in Mg-5Sr-2Mn-0.5Ce is ~ 0.15% higher than that in the Mg-3Sr-2Mn-0.5Ce alloy (Table 1), hence, the creep strengthening, can, in part, be attributed to the additional Ce.

For Mg-5Sr-2Mn-0.5Ce (JME521) at 200 °C under 50 MPa, the minimum creep rate was $2.78 * 10^{-10}$/s; this demonstrates higher creep performance than all available commercial alloys under similar conditions [2].

3.2. Microstructural evolution

3.2.1. Microstructural evolution upon isothermal treatment

Typical dendritic structures formed upon solidification in Mg-Sr-Mn-(Ce) alloys and the addition of 0.5% Ce to the ternary Mg-3Sr-2Mn alloy slightly refined the dendritic structure (Fig. 2a-c). Similar to the ternary Mg-Sr-Mn alloys, the increase in Sr content allowed more dendritic phase formation [7]. Ce is present in the dissolved state both within the matrix and interdendritic phases, whereas Mn is mainly concentrated in the intradendritic regions (Fig. 2c). The peritectic nature of Mn in Mg limited the concentration of Mn in the intradendritic regions. As previously reported, the as-cast microstructures of ternary Mg-Sr-Mn alloys with 3-5Sr and 2 Mn (wt%) consist of α-Mg matrix (supersaturated in Mn), primary α-Mn particles and $Mg_{17}Sr_2$ intermetallic phase in interdendritic regions [7,8]. The trace addition of Ce is found not to cause any new phase formation via XRD and EDS analyses (Fig. 2e). No precipitates were found in intradendritic regions in the as-cast condition.

No significant coarsening is observed in the interdendritic $Mg_{17}Sr_2$ phase upon annealing at 250 °C for 200 h, while the primary α-Mn phases increase in size consistent with the appearance of α-Mn peak in the XRD spectra (Fig. 2d and e). Upon isothermal treatment, the main change in microstructure is the precipitation from supersaturated α-Mg matrix in intradendritic regions. The intradendritic precipitation occurs with three distinct morphologies and size ranges in the annealed structures: (i) Rod-like precipitates (Fig. 3a and b) with their long axis either parallel or perpendicular to the basal plane of Mg (5–20 nm in width and 100–200 nm in length); (ii) Polygonal precipitates (~ 50 nm) with aspect ratio close to 1:1; and (iii) Thin plate-like precipitates with high aspect ratio (~ 1 μm in length and ~ 5 nm in width). Rod-like precipitates are distributed homogeneously in the matrix (Fig. 3a), and consist mainly of Mn with trace levels of Sr (EDS analysis – not shown). Polygonal and thin-plate precipitates are associated with each other (Fig. 3c) but have distinct elemental distribution as determined via high resolution EDS mapping. Thin-plates are Ce-rich precipitates, whereas polygonal particles are Mn-rich. Sr is also present in trace levels in the intra-dendritic regions with preferred concentration in precipitates consistent with its low solubility in Mg (0.11 wt% at 585 °C [13]).

Ce-rich precipitates: The equilibrium second phase is β-$Mg_{12}Ce$ in the Mg rich sides of the Mg-Ce system (for Ce < 32 wt%) and in the Mg-Ce-Mn system (for Ce < 25 wt%). Since no phase forms between Ce and Mn [13], Ce-rich precipitates with thin-plate morphology are likely the $Mg_{12}Ce$ phase. Long plate-like morphology was reported for $Mg_{12}Ce$ phase in numerous studies [6,12,14].

Mn-rich precipitates: These are α-Mn (Sr), consistent with the binary Mn-Sr phase diagram exhibiting the solubility limit of Sr in α-Mn as ~ 0.25 wt% at 700 °C [15]. The morphology, as well as, the

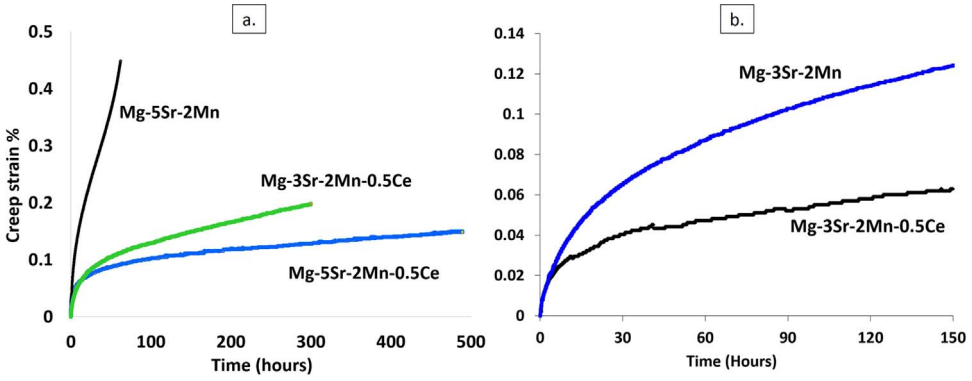

Fig. 1. Shows the creep results for two different conditions; (a) 200 °C, 50 MPa and (b) 175 °C, 40 MPa indicating the beneficial effect of trace additions of Ce in Mg-Sr-Mn alloys.